Submitted to Journal of the American Ceramic Society

LBL-6004
Preprint c.1

GRAIN BOUNDARY PHASES IN A HOT-PRESSED MgO SILICON NITRIDE

D. R. Clarke and G. Thomas

January 1977

Prepared for the U. S. Energy Research and Development Administration under Contract W-7405-ENG-48

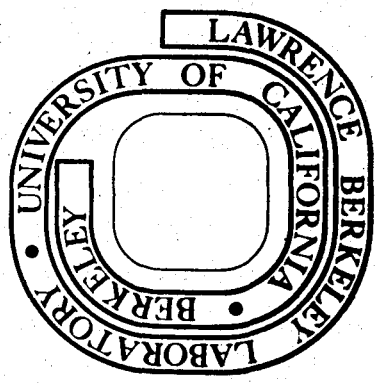

DISCLAIMER

GRAIN BOUNDARY PHASES IN A HOT-PRESSED MgO SILICON NITRIDE

D. R. Clarke and G. Thomas

Department of Materials Science and Engineering, College of Engineering and Materials and Molecular Research Division, Lawrence Berkeley Laboratory, University of California, Berkeley, California, 94720.

ABSTRACT

Although the high temperature loss of strength in ceramics such as silicon nitride has been attributed to the presence of intergranular amorphous phases, until now no direct proof has been offered. The present paper describes high resolution electron microscopy lattice imaging studies of a MgO hot-pressed silicon nitride from which it is concluded that intergranular second phases do indeed exist but they are heterogeneously distributed especially appearing at multiple grain junctions. These room temperature observations are compatible with the suspected microstructures at elevated temperatures.

Presented in part at the Pacific Coast Regional Meeting, The American Ceramic Society, San Francisco, Ca, November 3rd, 1976. (Basic Science Division, No 120-BEN-76 P)

I. Introduction

In many ceramics the properties, particularly the mechanical properties, are determined by their grain boundaries. These regions are of further interest since most ceramics are formed by either sintering or hot-pressing, both of which depend critically on the grain surfaces and boundaries. At the present the investigation of the grain boundaries in silicon nitride is particularly timely because of the intensive efforts in be USA, UK, Germany and Japan to demonstrate whether silicon nitride can truly be a structurally important material. One of the major problems preventing its application is the rather dramatic decrease in strength of the hot-pressed form above about 1000°C. This decrease is generally attributed to the presence of a glassy phase, between the individual silicon nitride grains, which, at high temperatures, rapidly decreases in viscosity with increasing temperature, flows and allows the grains to slide past one another. The glass is thought to be formed from the magnesium oxide fluxing aid used, the silica unavoidably present on the surfaces of the silicon nitride starting powders and the calcium oxide impurities in the silicon nitride.

Whilst this model, sometimes referred to as the "sand and molasses" model, is extremely attractive the experimental evidence for it is strictly circumstantial as no direct observation of a glassy phase in the grain boundary has been made. What evidence exists comes from what might be termed spatial "averaging" methods, methods where the information comes from a large number of grains at once. Auger electron spectroscopy of intergranular fracture surfaces [1,2], and the subsequent sputter ion etching, reveals the presence at the fracture surface of a layer with a composition identified as a magnesium calcium silicate. In these experiments the

information is averaged over an area of fracture surface of typically $3mm^2$. Internal friction measurements [3] show that there is a viscous component present in commercial grades of silicon nitride above about 800°C, which would be sufficient if it were a magnesium calcium silicate to form a continuous glassy boundary phase perhaps 50-1000 Å thick. Here the measurements are averaged over the entire volume of the specimens. Lastly, it has been found that using Y_2O_3 instead of MgO as the fluxing aid postpones the strength fall-off to higher temperatures [4]. This has been attributed to the formation of a more refractory grain boundary phase, but again the property measured is averaged over the entire volume of the material.

The present investigation was undertaken to observe directly whether the second phase does in fact lie between the individual grains as envisaged in the "sand and molasses" model or, if not, where in the microstructure it does exist. (The existence of a second phase is not in doubt since apart from the observations mentioned above, discrete amorphous regions commensurate in size to that of the grains have been seen by transmission electron microscopy.[5,6]) In order to do this the crystal lattice planes up to and on either side of selected grain boundaries have been directly observed using the technique of lattice fringe imaging with the transmission electron microscope. This technique makes it possible to study directly the structure of a crystalline material at an atomic level and has already proven to be extremely valuable in investigating phase transformations in metallic alloys[7,8] and the structure of a variety of minerals[9].

An advantage of the lattice fringe imaging technique is that the grain boundary phase can be either amorphous or crystalline and it will still be identifiable as a separate phase. This is important since the

second phase might be crystalline at room temperature and be viscous only at elevated temperatures. Such a situation would exist if the hot-pressed silicon nitride material were in fact near a eutectic as suggested by Lange[10]; the strength fall-off would correspond to the solidus temperature and grain sliding on a fluid layer could still occur above this temperature.

II. Experimental Details.

The material investigated was a Norton HS 130 silicon nitride prepared by hot-pressing with an addition of MgO to enhance densification and supplied by Dr. R. N. Katz, AMMRC. The material was examined in the virgin hot pressed condition.

Specimens for transmission electron microscopy were prepared in the standard manner: thin slices were cut from the hot-pressed billets using a diamond wheel, hand-ground to less than 50μm thickness, discs trepanned out and then finally ion-thinned. In order to produce extensive regions of very thin material necessary for lattice fringe imaging two additional precautions were taken. Firstly, the surfaces of the discs were diamond polished (0.25 μm grit) prior to ion thinning, and secondly the ion-thinning was carried out at a lower angle (~15°) than is customary. Finally, the thinned specimens were coated with a thin layer of evaporated carbon to prevent electrostatic charging under the electron beam.

The lattice fringe images were taken with a Philips EM301 electron microscope fitted with a high resolution stage. A magnification at the final screen of 450,000x was generally employed with the second condenser lens defocussed to double the exposure time from the fully focussed condition (a fully focussed condenser did not generally yield lattice fringe images). Exposure times were typically 16 or 32 seconds.

III. Boundary Selection.

In this section the conditions necessary for obtaining lattice fringe images and the selection of boundaries suitable for observation are both described. This is because fringe images can only be seen from adjacent grains when they are both in strong Bragg diffracting conditions and when the lattice spacing is larger than the resolution capabilities of the microscope.

Although lattice fringe imaging was first demonstrated in 1956[11] with the observation of the 12 Å lattice of pthalocyanine, its application in materials science has been restricted until the recent development of transmission electron microscopes with a line resolution of 2Å. In essence the method is the electron-optical analog of the Young's slit diffraction experiment in light-optics; the crystal planes diffract an incident illumination into a number of beams which can under prescribed conditions be made to interfere with one another to form a fringe pattern having the periodicity of the diffracting crystal planes. The details of the technique are described elsewhere[7,12], but in order to obtain a fringe image of a set of lattice planes in a crystal it is necessary to optimize the orientation of the crystal, its thickness, the precise diffracting conditions and microscope settings. Furthermore, in order to obtain a fringe image from two adjacent grains these experimental parameters must be optimized simultaneously and it is this restriction that limits which boundaries are suitable for such observation.

In the work described here the optimum conditions were established prior to the experiments by computation of the appropriate dynamical electron diffraction equations as will be described in a later publication. There are two main findings of these computations. Firstly, maximum fringe visibility for the majority of thicknesses in the range 50-500Å would

result when the crystals of silicon nitride are oriented such that basal or prism planes are strongly diffracting. Secondly, a thin second phase at a grain boundary can not be un-ambiguously identified if the boundary plane is inclined to the electron beam, and so the boundary must be observed edge-on.

On the basis of these considerations boundaries suitable for observation were selected as follows. Firstly, with the microscope operating in the diffraction mode, the thinned specimen was translated under the beam until two adjacent grains were found to be diffracting strongly. Then the microscope was switched to the imaging mode to observe whether the boundary plane was parallel to the electron beam.

In order to obtain a lattice fringe image from each grain, transmitted and diffracted beams suitably tilted with respect to the microscope axis were selected with the objective aperture, as shown schematically in figure 1. The objective lens defocus and astigmatism were then adjusted until the diffraction images on the screen coincided. At this condition the objective lens was over-focused from the usual criterion for judging focus (the disappearance of the Fresnel fringe at the specimen edge), and well defined, high visibility fringes could be recorded.

IV. Observations.

A number of representative lattice fringe images of grain boundary regions are presented in this section to illustrate the various types of boundary and second phase morphologies observed in the hot pressed silicon nitride. In each micrograph the boundary plane is seen edge on.

Figure 2 is an example of the commonest type of grain boundary regions seen, and is in this case a small angle (~11°) boundary between two alpha silicon nitride grains. Here the lattice fringes can be followed right up to the boundary from either side and the only discontinuity in

fringes is the boundary itself. This shows that if a second phase is present at the boundary it must certainly be less than one interplanar distance wide in projection, which in this example would mean less than 6.7Å. Also the boundary structure itself is of interest because it is facetted and each facet is one $d_{(10\bar{1}0)}$ spacing high.

In a number of instances a discontinuity, presumably a second phase can be seen in a grain boundary and an example is presented in figure 3. In this case the boundary is a high angle grain boundary with one set of prism planes being imaged in both α grains. The second phase here is at most 7Å thick and is, remarkably, of almost constant thickness along the entire length of the boundary (~2500Å). This constant thickness probably results from the fact that the boundary plane coincides with the prism plane of the right hand grain and with the exception of the interplanar-spacing-high step at A, the boundary is atomically flat along its entire length. Such a constant thickness when the boundary orientation remains constant indicates that the two phases have reached some sort of equilibrium. The presence of isolated steps such as the one at A was characteristic of all the boundaries where the boundary plane was formed by a low index plane and suggests that densification during hotpressing occurs by a ledge migration mechanism.

The dark shadowy appearance at the grain edges is a contrast effect which appears likely to have resulted from a thickness change due to a slight preferential etching occurring at the grain boundaries, since the extent of the shadow alters as the objective lens defocus was changed.

However, apart from observations of these thin layers the intergranular second phases were observed only at multiple grain junctions, and an example is shown in figure 4a. The junction is between two alpha grains and an un-identified grain. The second phase gradually tapers down from the triple point, where it has maximum width, until it becomes impos-

sible to identify and the adjacent grains abut with one another. The end of the wedge is shown at higher magnification in fig. 4b and it is clear from following the lattice fringes in the two adjacent grains that the second phase decreases in width until it can no longer be detected in the lattice image and the boundary is then similar in morphology to that of figure 2a.

Another example of a three point junction is that of figure 5. The very dark grain on the left is out of contrast and cannot be identified but the broad, faint and widely spaced fringes at B are Moire fringes indicating that it is crystalline as the other two grains are. The second phase at A is located at the junction of the three grains. The curved shape of the second phase is indicative that it has "wet" the three grains during the hot-pressing of the material, and is extremely suggestive of once being fluid. It also appears to have wet the boundaries to the left and to the right of the triple point since it can be seen to run down these boundaries.

In addition to the specific features illustrated above the lattice fringe images also show a number of general features. Firstly, the grain boundaries often appear to be very straight as in fig.3 or made up of short straight facets as in figure 2. The preponderance of (10T0) faces would suggest that this is the lowest energy surface face in silicon nitride. Secondly, the spacing of the lattice fringes, as measured both directly on the negative and by optical diffraction from the negative, right up to the boundary plane is constant within the measurable accuracy (~3%). This implies that if segregation of solute to the grain boundary regions is occurring then the solute does not cause a lattice parameter change greater than 3%.

V. Discussion.

Since the size of the area examined when taking a lattice fringe image is so small, typically 2000Å x 2000 Å square, there is a severe statistical problem in generalizing from the observations made of selected boundaries to the character of the boundaries throughout a specimen. Never-the-less, these observations do show that at room temperature there does not exist a continuous second phase between all individual grains in hot-pressed silicon nitride as envisaged by the "sand and molasses" model. The results also indicate that the second phase is generally localized at the three-grain junctions, and a number of micrographs such as fig. 3 suggest that there may, in a few instances, be a very thin layer of second phase between grains.

Furthermore it is felt that the observations are of representative boundaries since they were selected essentially at random. Firstly, no preference for orientation was made when the specimens were cut from the billet. Secondly, since it was not possible to tilt the specimens in this microscope so as to bring any boundary into the required diffracting conditions, the specimens were translated until a boundary was observed satisfying the necessary diffraction conditions. This operation was carried out with the microscope in the diffraction mode, so the microstructure was not seen until after a suitable boundary had been found. The probability of finding such a boundary region in this manner is then equivalent to the chance of finding a specific orientation in a section through a randomly oriented collection of grains. The diffraction conditions stipulated for the observation of fringes from adjacent grains do not imply any non-randomness either, since they only refer to the way in which the boundary is observed with respect to the incident electron beam.

It is realized that the observations reported here were made at room temperature whilst the strength degradation actually occurs at a high temperature where the microstructure may be different. However, the observed microstructure and the "sand and molasses" behavior at elevated temperatures need not be incompatible and may be rationalized on the basis of a temperature dependent wetting of the silicon nitride grains by the second phase. The "sand and molasses" behavior implies that the second phase wets the silicon nitride at the temperatures at which the strength degradation occurs, i.e. the surface tension between the second phase and the silicon nitride $2\gamma_{LS}$ is less than the surface tension between two silicon nitride grains $2\gamma_{ss}$. As the temperature is lowered both surface tensions γ_{LS} will increase at a faster rate than γ_{ss} since by its very nature the entropy of the viscous second phase - silicon nitride interface will decrease faster than the entropy associated with the solid-state interface between two silicon nitride grains. Thus at some temperature γ_{LS} will become greater than γ_{ss} and the second phase will no longer wet the silicon nitride grains and withdraw from between the grains. As the surface tensions will be a function of the crystallographic orientation of the silicon nitride boundaries the temperature at which wetting no longer becomes favorable will vary with orientation. So at room temperature the second phase would be expected to have withdrawn from many but not necessarily all boundaries and to be concentrated at three and four grain junctions, as observed.

On the basis of such a temperature dependent wetting model the presence of a second phase on a fracture surface will be a function of the temperature at which the material is broken. In fracturing above about 1000°C it is expected that the fracture surface would be covered by the second phase since all the silicon nitride grains are wet. At room temperature

all the grains would not be wet and it is unlikely that the entire fracture surface would be covered with second phase. It would then only be present on those grains which had remained wetted and at some of the three grain junctions. In the Auger Spectroscopy experiments reported to date[1,2] such differences could not be detected since the Auger electron signal was collected from tens of thousands of grains at once.

Whilst the lattice fringe imaging of grain boundary regions enables the presence of a second phase to be established the technique imposes two limitations on the identification of the phase. Firstly, it is not possible to image details smaller than the interplanar spacing of the crystal lattice, so if a second phase having a width of less than a lattice spacing were present at the boundary it could not be detected. Secondly, it is not possible to determine whether a thin second phase is amorphous or crystalline except in the special instance where it is both crystalline and oriented to give lattice fringes.

VI. Conclusions

I) Using the lattice fringe image technique it has been possible to observe for the first time the grain boundary region of a ceramic material at the atomic level.

II) The observations of a MgO hot-pressed silicon nitride indicate that at room temperature the second phase does not exist as a continuous wetting layer at the grain boundaries, but rather is generally localized at some of the three grain junctions and on occasions as a very thin (<10 Å) layer between two grains.

Acknowledgements

This work has been supported by the National Science Foundation through the Division of Materials Research (D.R.C.) and by the United States Energy Research and Development Administration through the Materials and Molecular Research Division of the Lawrence Berkeley Laboratory. We are grateful to Dr. R. N. Katz of the Army Materials and Mechanics Research Center, Watertown for kindly supplying the silicon nitride specimens.

References

1. R. Kossowsky, "The Microstructure of Hot-Pressed Silicon Nitride," J. Mater. Sci., 8 (11), 1603-1615, (1973).

2. B. D. Powell and P. Drew, "The Identification of a Grain Boundary Phase in Hot-Pressed Silicon Nitride by Auger Electron Spectroscopy," J. Mater. Sci. 9 (11), 1867-1870, (1974).

3. D. R. Mosher, R. Raj and R. Kossowsky, "Measurement of Viscosity of the Grain Boundary Phase in Hot-Pressed Silicon Nitride," J. Mater. Sci.. 11 (1), 49-53 (1976).

4. G. E. Gazza, "Hot Pressed Silicon Nitride," J. Amer. Ceram. Soc. 56 (12), 662, (1973).

5. A. G. Evans and J. V. Sharp, "Microstructural Studies on Silicon Nitride" J. Mater. Sci., 6 (10) 1292-1302, (1971).

6. P. Drew and M. H. Lewis, "The Microstructures of Silicon Nitride Ceramics during Hotpressing Transformations," J. Mater. Sci. 9 (2), 261-269 (1974).

7. R. Sinclair, K. Schneider and G. Thomas, "Analysis of Ordering in Cu_3Au Utilizing Lattice Imaging Techniques," Acta. Met. 23 (7), 873-883, (1975).

8. R. Sinclair, R. Gronsky and G. Thomas, "Optical Diffraction from Lattice Images of Alloys," Acta Met. 24(9), 789-796 (1976).

9. "Electron Microscopy in Mineralogy," edited by H-R. Wenk, Springer-Verlag, New York, (1976).

10. F. F. Lange, "Dense Silicon Nitride: Interrelation between Phase Equilibria Microstructure and Mechanical Properties," Final Technical Report, ARPA Contract N00014-74-C-0284, Westinghouse Electric Corp. 1976.

11. J. W. Menter, " The Direct Study by Electron Microscopy of Crystal Lattices and Their Imperfections," Proc. Roy. Soc. A326, 119-135 (1956).

12. J. G. Allpress and J. V. Sanders, " The Direct Observation of the Structure of Real Crystals by Lattice Imaging," J. Appl. Cryst. 6 (2) 165-190 (1973).

Figure Captions

Fig. 1 The position of the objective aperture with respect to the diffraction pattern for lattice fringe imaging. Schematic Illustration.

Fig. 2 Lattice fringe image of a small angle boundary between two alpha silicon nitride grains. The fringes can be followed right up to the boundary from either side indicating the absence of a second phase in the grain boundary. α - Si_3N_4 (10T0) spacing is 6.7Å .

Fig. 3 A thin second phase is present at the grain boundary here since the lattice fringes do not continue right up to the boundary. The second phase is of almost constant thickness along the entire length of the boundary with the exception of the 6.7Å step at A.

Fig. 4 a) A wedge-shaped second phase at a three grain junction revealed by imaging the lattice fringes in the adjacent α -Si_3N_4 grains. b) Higher magnification image showing that the second phase decreases in thickness until the adjacent grains abut against one another.

Fig. 5 A three grain junction. The lattice fringes indicate that the second phase is concentrated at the junction, A, forms a thin layer between the grains leading from the junction. The dark grain on the left is out of contrast, but the Moire fringes at B indicate that it is crystalline.

Figure Captions

Fig. 1 The position of the objective aperture with respect to the diffraction pattern for lattice fringe imaging. Schematic Illustration.

Fig. 2 Lattice fringe image of a small angle boundary between two alpha silicon nitride grains. The fringes can be followed right up to the boundary from either side indicating the absence of a second phase in the grain boundary. α - Si_3N_4 (10T0) spacing is 6.7Å .

Fig. 3 A thin second phase is present at the grain boundary here since the lattice fringes do not continue right up to the boundary. The second phase is of almost constant thickness along the entire length of the boundary with the exception of the 6.7Å step at A.

Fig. 4 a) A wedge-shaped second phase at a three grain junction revealed by imaging the lattice fringes in the adjacent α -Si_3N_4 grains. b) Higher magnification image showing that the second phase decreases in thickness until the adjacent grains abut against one another.

Fig. 5 A three grain junction. The lattice fringes indicate that the second phase is concentrated at the junction, A, forms a thin layer between the grains leading from the junction. The dark grain on the left is out of contrast, but the Moire fringes at B indicate that it is crystalline.

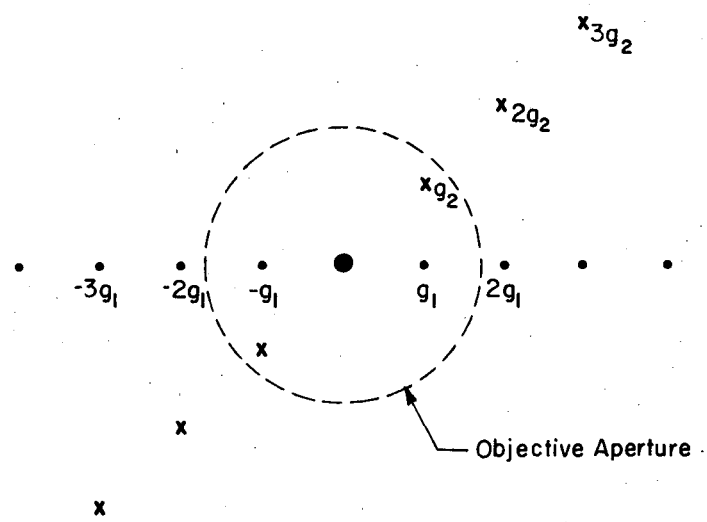
$3g_2$
$2g_2$
g_2
$-3g_1$
$-2g_1$
$-g_1$
g_1
$2g_1$
Objective Aperture
XBL 7612-11,026

FIG. 1

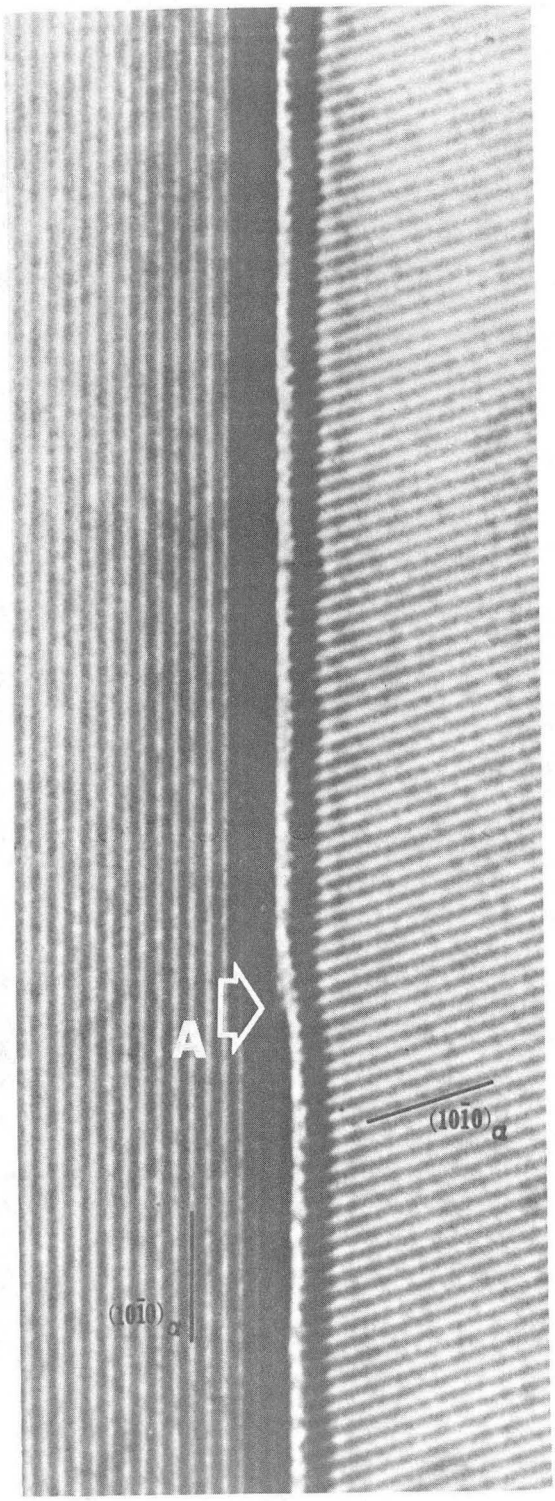

XBB 760 11300A

FIG. 3

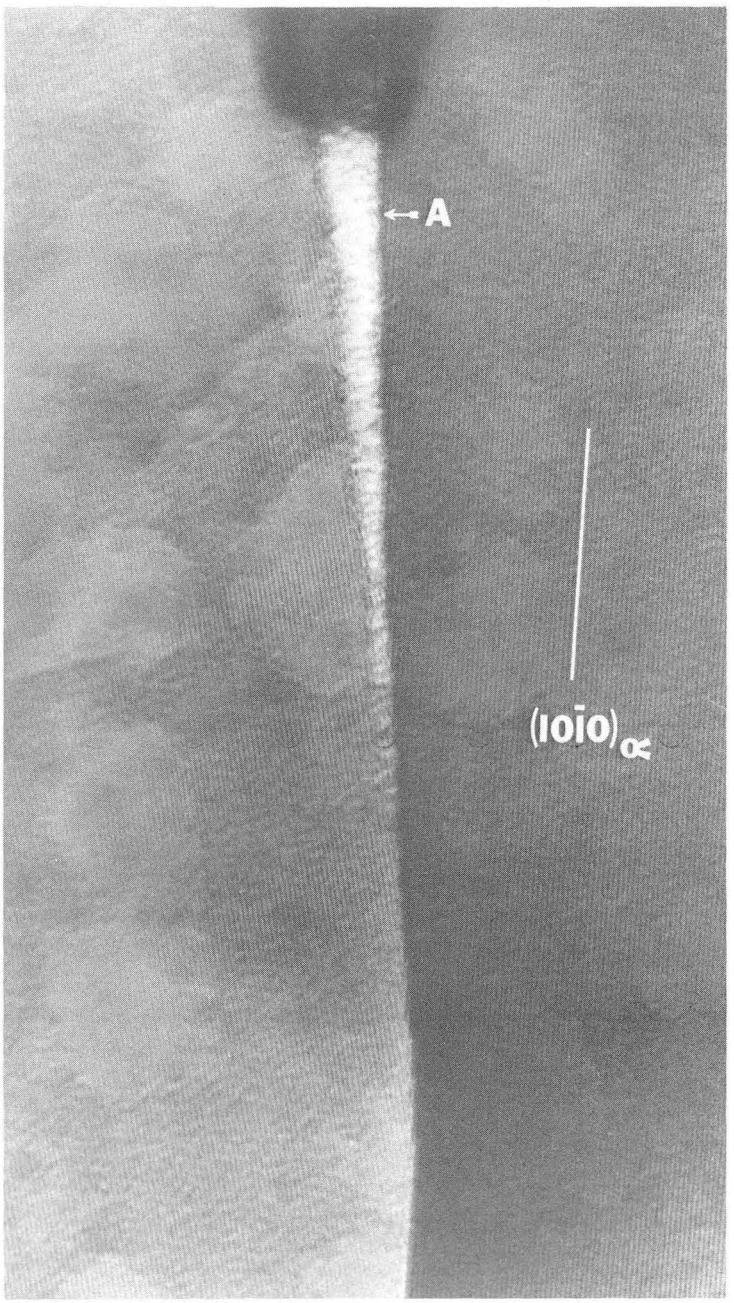

XBB 760 9732

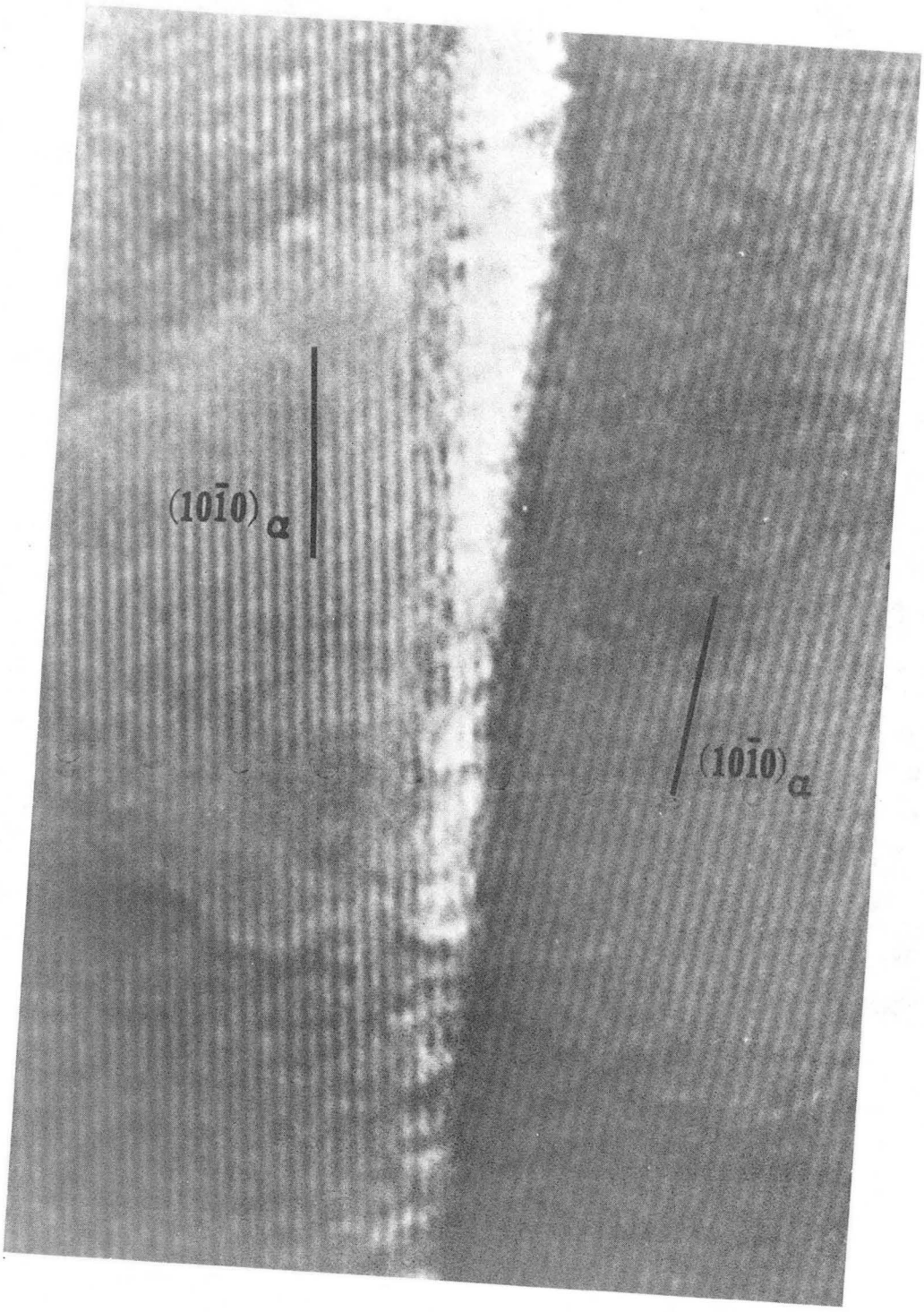

XBB 760 11299A

FIG. 4b

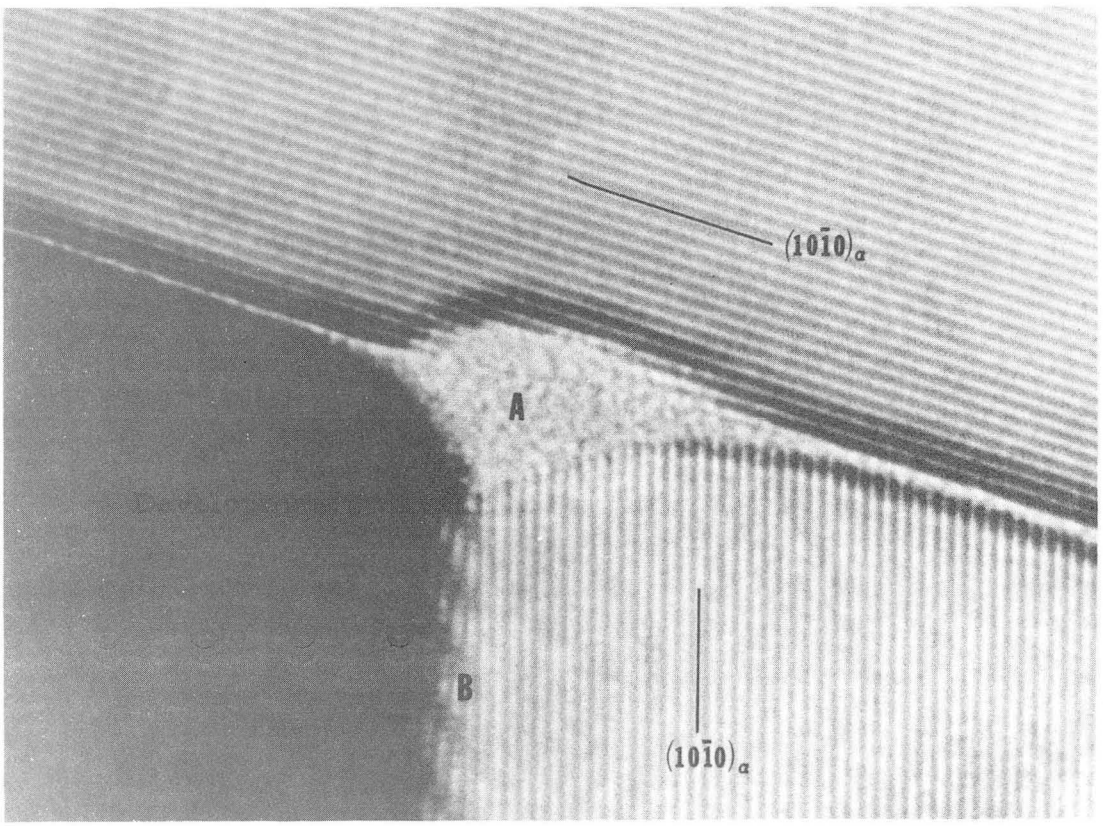

XBB 769 8516

FIG. 5

This report was done with support from the United States Energy Research and Development Administration. Any conclusions or opinions expressed in this report represent solely those of the author(s) and not necessarily those of The Regents of the University of California, the Lawrence Berkeley Laboratory or the United States Energy Research and Development Administration.

TECHNICAL INFORMATION DIVISION
LAWRENCE BERKELEY LABORATORY
UNIVERSITY OF CALIFORNIA
BERKELEY, CALIFORNIA 94720